Extraction of the Hemodynamic Response in Randomized Event-Related Functional MRI

Narter Ari and Yi-Fen Yen

Department of Medical Engineering, Wake Forest University School of Medicine, Winston-Salem, NC, USA

Abstract— **Signal detection in noisy data set is a common problem in signal processing. Detection of the hemodynamic response function (HRF) embedded in randomized event-related fMRI (rER-fMRI) time series is an example of this problem. So far, most studies that set out to obtain *unbiased* HRF use some forms of time-window (TW) averaging method to extract HRF from the rER-fMRI data. In this paper we applied two methods, Cepstral Analysis and Conjugate Gradients (CG) for Deconvolution to extract HRF. These methods depend only on the knowledge of when events occured and do not require any apriori information about the HRF. These methods and the popular TW averaging method are tested on simulated data, as well as *in vivo* data obtained from rER-fMRI experiments. All three methods identified timing of HRF accurately, but only CG for Deconvolution method was robust in reproducing the shape under varying experimental conditions.**

Keywords— **fMRI; Event-related; Hemodynamic response; MRI; Conjugate Gradients; Cepstrum; ISI.**

I. Introduction

The randomized event-related fMRI (rER-fMRI) experimental designs have become increasingly popular in recent years as the designs have drastically improved efficiency [1] over the fixed inter-stimulus interval (ISI) designs. The rER-fMRI designs allow different stimuli to be presented in random sequences and timing, and thus, eliminating potential confounds caused by anticipation, habituation, or other strategy effects [2].

The fMRI signal is caused by changes in blood oxygenation and blood volume that result from the neural activity induced by the stimuli. The timing characteristics of this vascular response, or the hemodynamic response function (HRF), can be extracted from the rER-fMRI data assuming linearity between the fMRI signal and the underlying neuronal activity. The linearity has been demonstrated by various studies [3]-[5] in the intermediate ISI range (2-15s), but not always true for short ISI [6].

So far, most studies that set out to obtain *unbiased* HRF use some forms of time-window (TW) averaging method to extract the HRF from the rER-fMRI data. We found that the TW averaging method could be unreliable, depending on the mean ISI (mISI) and randomness. The goal of this study was to develop robust algorithms to extract HRF with better accuracy than the TW averaging method.

II. Materials and Methods

A. Theories

By assuming a linear time-invariant model for the observed fMRI response, rER-fMRI signal $y(t)$ can be modeled as the convolution $y(t) = s(t) \star h(t)$ of the HRF $h(t)$

N. Ari E-mail: nari@wfubmc.edu

and event onset time series $s(t)$, which is represented as a series of impulses, $s(t) = [10010..]$.

A.1 Time Window Averaging

TW averaging is a common method used to extract the HRF [7]. HRF is estimated by using a fixed time window starting with each stimulus and then averaging the signals measured within each of these time windows. The idea is to increase low signal to noise ratio of rER-fMRI signals by averaging.

A.2 Cepstral Analysis

Cepstral analysis, a nonlinear signal processing technique, is commonly applied to signals that have been combined by convolution, such as in speech processing and homomorphic filtering [8]. Complex cepstrum (CCeps) of $x(t)$ can be calculated by taking logarithm of the FFT of $x(t)$ and applying inverse FFT to the result. The transformation of a signal into its CCeps enables us to use an operation that has the same algebraic properties as addition, instead of using multiplication in the frequency domain.

We were able to extract $h(t)$ via cepstral analysis by subtracting the CCeps of $s(t)$ from the CCeps of $y(t)$ and taking the inverse CCeps of the result. Then a low-pass filtering was applied to obtain a smooth HRF.

$$
\begin{aligned}
y(t) &= s(t) \star h(t) & TimeDomain \\
Y(f) &= S(f).H(f) & FrequencyDomain \\
log\big(Y(f)\big) &= log\big(S(f)\big) + log\big(H(f)\big) \\
F^{-1}\{log(H(f))\} &= F^{-1}\{log(Y(f))\} - F^{-1}\{log(S(f))\} \\
CCeps[h(t)] &= CCeps[y(t)] - CCeps[s(t)] \\
h(t) &= CCeps^{-1}\{CCeps[y(t)] - CCeps[s(t)]\}
\end{aligned}
$$

A.3 Conjugate Gradients (CG) for Deconvolution

The CG method is an iterative method for solving a linear system of equations $Ax = b$, with symmetric positive definite (SPD) coefficient matrix A. However, with simple modifications this method can be applied to nonsymmetric and overdetermined least-squares problems [9].

Following the previous notation, convolution can be expressed as $Y(f) = S(f).H(f)$ in the Fourier domain. In order to solve the deconvolution problem of extracting HRF, we applied the CG algorithm [9], [10] to compute a least-squares solution, (see the detailed algorithm in the Appendix)

$$
\min_{H(f)} \parallel Y(f) - S(f).H(f) \parallel_2
$$

Report Documentation Page

Report Date 25 Oct 2001	Report Type N/A	Dates Covered (from... to) -

Title and Subtitle Extraction of the Hemodynamic Response in Randomized Event-Related Functional MRI	**Contract Number**
	Grant Number
	Program Element Number
Author(s)	**Project Number**
	Task Number
	Work Unit Number
Performing Organization Name(s) and Address(es) Department of Medical Engineering Wake Forest University School of Medicine Winston-Salem, NC	**Performing Organization Report Number**
Sponsoring/Monitoring Agency Name(s) and Address(es) US Army Research, Development & Standardization Group (UK) PSC 802 Box 15 FPO AE 09499-1500	**Sponsor/Monitor's Acronym(s)**
	Sponsor/Monitor's Report Number(s)

Distribution/Availability Statement Approved for public release, distribution unlimited
Supplementary Notes Papers from 23rd Annual International Conference of the IEEE Engineering in Medicine and Biology Society, October 25-28, 2001, held in Istanbul, Turkey. See also ADM001351 for entire conference on cd-rom.
Abstract
Subject Terms

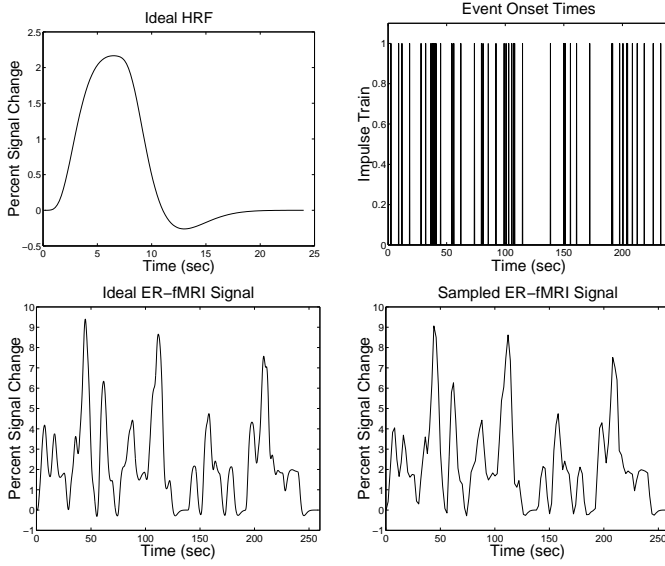| **Report Classification** unclassified	**Classification of this page** unclassified
Classification of Abstract unclassified	**Limitation of Abstract** UU

Number of Pages 4

Fig. 1. Simulated rER-fMRI signal with 5s mISI, generated by convolving the ideal HRF with the event onset time series and sampling at 2s interval.

B. Simulations

An ideal HRF [11] was used as the impulse response function of the model. The stimulus onset time series were generated with randomized ISI for a given mISI. Then the ideal rER-fMRI signal was simulated by convolving the ideal HRF and the stimulus onset time series (Fig .1). Finally the ideal rER-fMRI signal was sampled at an interval of 2s, the same as the repetition time (TR) used in the fMRI experiments. All simulation data were kept within a total time series of 240s.

Two types of simulations were performed to compare the three HRF extraction algorithms. First, simulated data with different mISI values: 2s, 5s and 10s, were used to test the sensitivity of the HRF extraction algorithms to a range of mISI. Secondly, simulated data with 5s mISI but different randomness were used to test the stability of the three methods.

C. rER-fMRI experiments

The five stimulus onset time series (2s, 5s, and 20s mISI, and the additional two 5s mISI series with different randomness) implemented for the simulation data were used to construct visual stimulation paradigms for the rER-fMRI experiments. Each stimulus consists of a black-and-white checkerboard displayed for 250ms at every event onset time. The experiments were performed on a clinical 1.5T MRI scanner by using a T2* gradient-echo 2D spiral sequence with TR of 2s. Twenty slices were acquired per TR to cover the whole brain. The spatial resolution was 3.75mm X 3.75mm X 7mm.

The fMRI data were processed and analyzed by using Statistical Parametric Mapping [11]. The image volumes were adjusted for slice-timing, realignment, normalization, and smoothing prior to statistical analysis for the significance of activation. In order to obtain meaningful fMRI
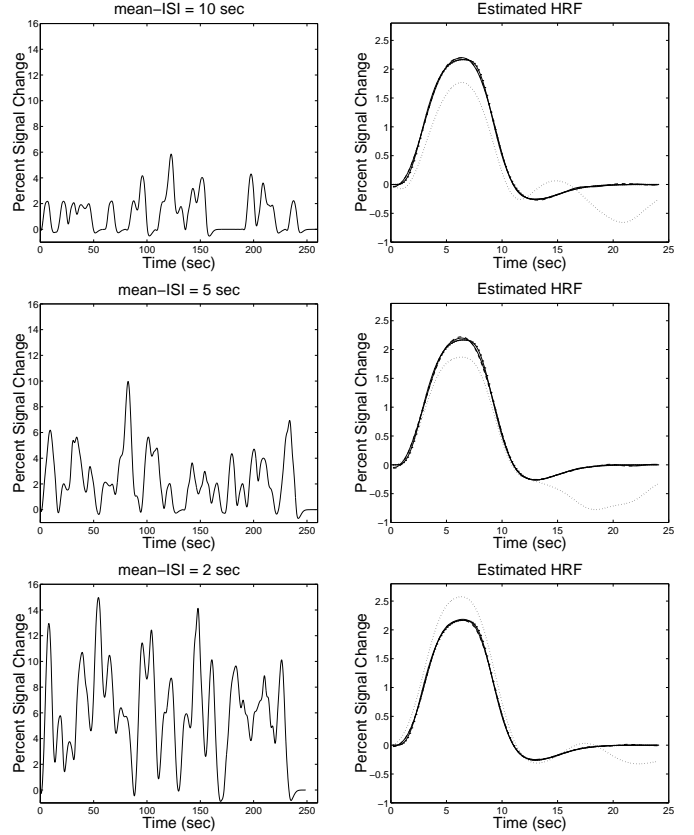

Fig. 2. (Simulation) The effect of decreasing mISI on HRF extraction algorithms. Simulated signal time courses are shown on the left column. Results of the HRF extraction algorithms are plotted on the right column. The ideal HRF (dot-dashed) is reproduced very well by the Cepstral Analysis (dashed) and the CG for Deconvolution (solid) methods, but not very well by the TW Averaging (dotted) method.

response for the comparison of the algorithms, three adjacent voxels with significant activation (t-score > 4) were identified at the same location in the primary visual cortex from all data sets. The raw time course was temporally smoothed by a zero-mean Gaussian with 2s standard deviation. The average time course of the three voxels for each data set was used to extract HRF with the three proposed methods. Note that these methods were also robust for a single voxel time-course analysis.

III. RESULTS

A. Simulations

Cepstral Analysis and CG for Deconvolution methods worked almost perfectly for the zero-noise, simulated rER-fMRI signals for mISI of 2s, 5s, and 10s (Fig. 2). Maximum mean-square errors (MSE) were calculated as 0.15 and 0.09 for the Cepstral Analysis and CG for Deconvolution methods, respectively. On the other hand, results of TW Averaging method were unstable. MSE was calculated as high as 20.51 for 5s mISI. Also undershooting or overshooting of the peak was observed for all cases.

Cepstral Analysis and CG for Deconvolution methods were very robust for 5s mISI of various randomness (Fig.
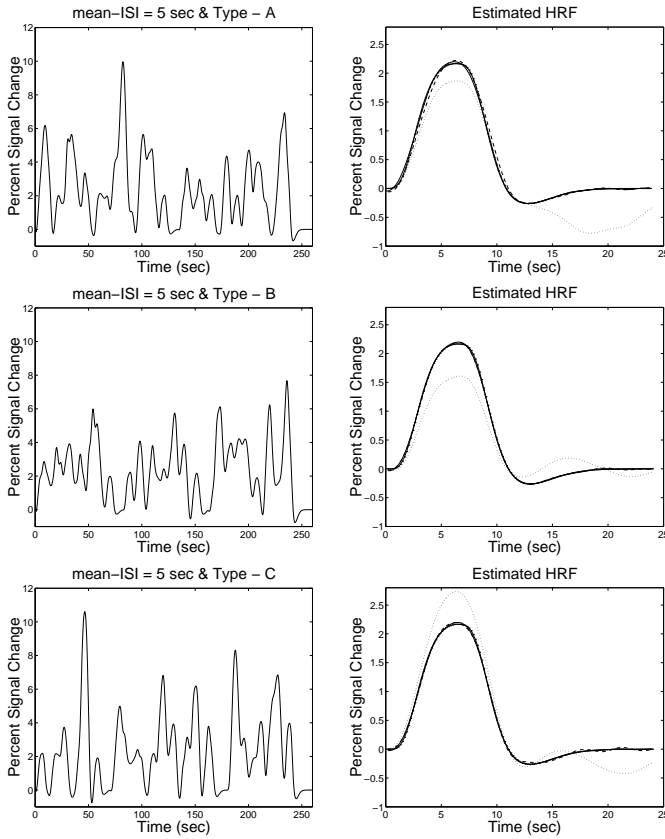
Fig. 3. (Simulation) The effect of changing randomness on HRF extraction algorithms. Simulated signal time courses for 5s mISI are shown on the left column. Results of the HRF extraction algorithms are plotted on the right column with the same line style notations as those in Fig.2. The TW Averaging method produces the least accurate results among the three methods.
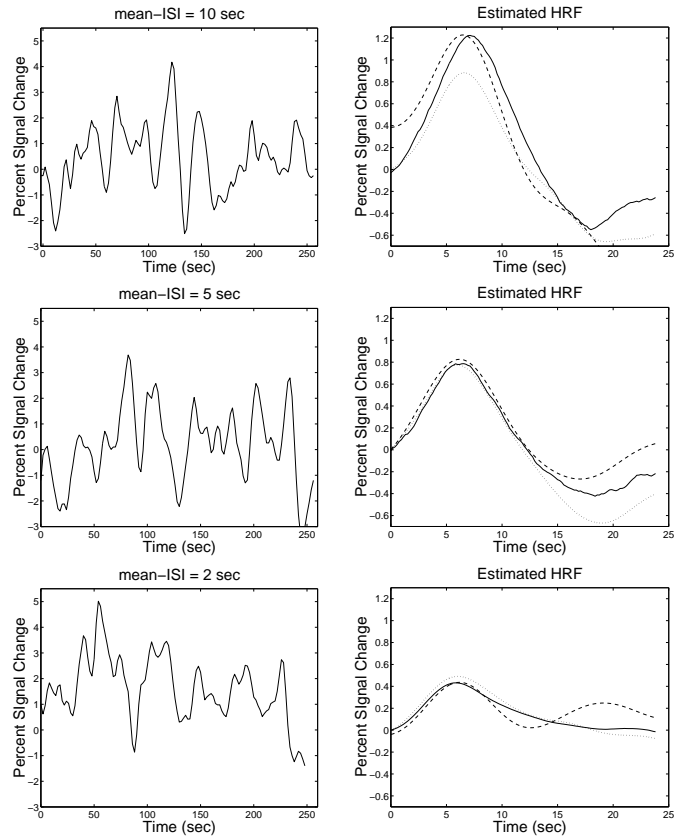
Fig. 4. (*In vivo* data) The effect of decreasing mISI on HRF extraction algorithms. The *in vivo* time courses are shown on the left column. Results of the HRF extraction algorithms are plotted on the right column with the same notations as those in Fig.2. Note that the result of Cepstral Analysis for 10s mISI was cut at -0.7, although it has a minimum value of -1.1

3) with maximum MSE values 0.15 and 0.09, respectively. But the performance of the TW Averaging method was unstable even for the same mISI. From simulations, we found that TW Averaging performs well in estimating time-to-peak (TTP) of HRF, but the method is not reliable in reproducing the shape, such as maximum percentage change (MPC) and full-width at half maximum (FWHM).

B. In Vivo

The MPC, TTP, and FWHM values extracted from the *in vivo* data, are listed in Table 1 for all methods. The methods were consistent (Fig. 4) in estimating the TTP, but their results differed in estimating the shape of HRF as in simulations. For 2s mISI, the MPC of TW Averaging was greater than the MPC of the other two methods, which is consistent with the overshooting of the peak observed in simulations. For 5s and 10s mISI, the MPC of TW Averaging was less than the MPC of the other two methods, which is also consistent with the undershooting of the peak observed in simulations.

For the 5s mISI data sets of various randomness, extracted TTP was in agreement (Fig. 5) among the three methods (mean±SD = 5.93±0.14, 5.93±0.16, and 5.94±0.18). But they differed in estimating the shape of

the HRF. Undershooting or overshooting behaviour of the peak from the TW Averaging method was similar to the simulation results. Note that the Cepstral Analysis did not converge to zero for type-C randomness. The CG for Deconvolution method maybe more robust than other methods in that the standard deviations of MPC (0.09) and FWHM (0.38) from the three randomness data sets were the smallest among the three methods.

IV. Conclusions

Our main finding is that all methods accurately identified the TTP of the HRF, but only the CG for Deconvolution method was reliable in estimating the shape under varying experimental conditions. The TW Averaging was the least robust in estimating the shape of the HRF in both the simulation and *in vivo* data. Cepstral Analysis worked well for the zero-noise, simulated rER-fMRI signals, however it was unstable in the presence of noise. The CG for Deconvolution method performed the best both in simulations and in vivo applications. Since it is an iterative method, it handled noise better than the Cepstral Analysis. We concluded that the CG for Deconvolution method is a reliable and robust method, and it is a strong alternative to the commonly used TW Averaging method.

TABLE I

MPC, TTP, AND FWHM OF EXTRACTED HRF FROM *In Vivo* DATA FOR DIFFERENT MEAN-ISI VALUES

mean-ISI	Cepstral Analysis			TW Averaging			CG for Deconvolution		
(sec)	MPC (%)	TTP (sec)	FWHM (sec)	MPC (%)	TTP (sec)	FWHM (sec)	MPC (%)	TTP (sec)	FWHM (sec)
10	1.23	6.49	7.10	0.88	6.61	6.15	1.22	7.08	6.90
5	0.83	6.19	7.10	0.77	6.01	6.57	0.79	6.08	6.61
2	0.44	6.19	6.12	0.49	6.04	7.66	0.43	5.82	7.42
5 type-A	0.78	6.00	7.08	0.72	5.90	6.66	0.75	5.96	6.76
5 type-B	0.62	6.03	6.15	0.49	5.79	5.91	0.68	5.75	6.06
5 type-C	0.51	5.77	6.93	0.69	6.10	6.64	0.58	6.11	6.66
mean±SD	0.64±0.14	5.93±0.14	6.72±0.50	0.63±0.13	5.93±0.16	6.40±0.43	0.67±0.09	5.94±0.18	6.49±0.38

MPC = maximum percentage change; TTP = time-to-peak; FWHM = full width at half maximum.
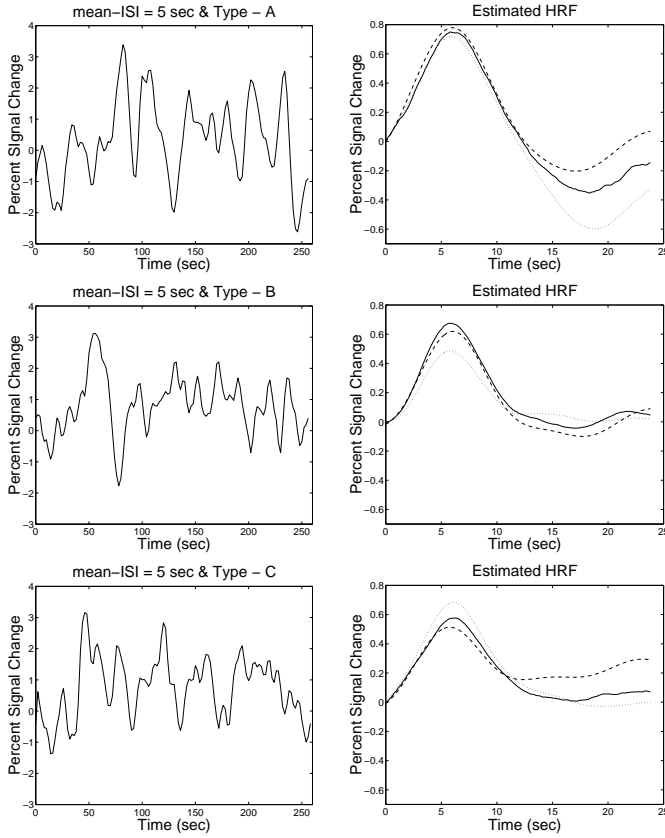

Fig. 5.   (*In vivo* data) The effect of changing randomness on HRF extraction algorithms. The *in vivo* time courses for 5s mISI are shown on the left column. Results of the HRF extraction algorithms are plotted on the right column with the same notations as those in Fig.2.

APPENDIX

A. CG for Deconvolution Algorithm

Inputs y: n x 1 signal vector, s: k x 1 impulse train vector.

Output h: m x 1 least squares solution to $y = s \star h$.

$\quad h = ones(m, 1) \qquad \rightarrow$ initialize h

$\quad \underline{h} = [h; zeros(n - m, 1)], \qquad \underline{s} = [s; zeros(n - k, 1)]$

$\quad y_f = fft(y, n), \qquad \underline{h}_f = fft(\underline{h}, n), \qquad \underline{s}_f = fft(\underline{s}, n)$

$\quad S_f = \underline{s}_f^c \odot \underline{s}_f + \nu$

$\quad \underline{r}_f = \underline{s}_f^c \odot y_f - S_f \odot \underline{h}_f$

$\quad \underline{r} = ifft(\underline{r}_f), \qquad r = \underline{r}(1 : m), \qquad p = -r$

$while \parallel r \parallel / \parallel y \parallel > \epsilon$

$\quad \underline{p} = [p; zeros(n - m, 1)], \qquad \underline{p}_f = fft(\underline{p}, n)$

$\quad \underline{w}_f = S_f \odot \underline{p}_f, \qquad \underline{w} = ifft(\underline{w}_f), \qquad w = \underline{w}(1 : m)$

$\quad \alpha = r^T r / p^T w$

$\quad h = h - \alpha p$

$\quad r_{old} = r, \qquad r = r_{old} + \alpha w$

$\quad \beta = r^T r / r_{old}^T r_{old}$

$\quad p = -r + \beta p$

$end(while)$

B. Implementation Details

In CG for Deconvolution algorithm, we used the following MATLAB notation. $y_f = fft(y, n)$ is n-point FFT of vector y. $\underline{h} = [h; zeros(n - m, 1)]$ means to pad zeros at the bottom of vector h. $\odot$ denotes component-wise multiplication. h^c denotes component-wise complex conjugate of vector h. ν represents the regularization parameter.

REFERENCES

[1] A. M. Dale, "Optimal experimental design for event-related fMRI," *Hum. Brain Mapp.,* vol. 8(2-3), pp. 109-114, 1999.

[2] B. R. Rosen, R. L. Buckner and A. M. Dale, "Event-related functional MRI: past, present, and future," *Proc. Natl. Acad. Sci. USA,* vol. 95(3), pp. 773-780, 1998.

[3] G. M. Boynton, S. A. Engel, G. H. Glover and D. J. Heeger, "Linear systems analysis of functional magnetic resonance imaging in human V1," *J. Neuroscience,* vol. 16(13), pp. 4207-4221, 1996.

[4] A. M. Dale and R. L. Buckner, "Selective averaging of rapidly presented individual trials using fMRI," *Hum. Brain Mapp.,* vol. 5, pp. 329-340, 1997.

[5] S. Pollmann, C. J. Wiggins, D. G. Norris, D. Y. von Cramon and T. Schubert, "Use of short intertrial intervals in single-trial experiments: a 3T fMRI-study," *Neuroimage,* vol. 8(4), pp. 327-339, 1998.

[6] K. J. Friston, O. Josephs, G. Rees and R. Turner, " Nonlinear event-related responses in fMRI," *Magn. Reson. Med.,* vol. 39(1), pp. 41-52, 1998.

[7] O. David, J. Warnking and C. Segebarth, "Event-related fMRI with pseudo-randomized inter-stimulus intervals (ISI). Optimization of the distribution of the ISI," *Proc. Intl. Soc. Mag. Reson. Med. 2000,* vol. 8, p. 58.

[8] A. V. Oppenheim and R. W. Schafer, *Discrete-Time Signal Processing,* Intl. ed. Englewood Cliffs, NJ: Prentice-Hall, 1989.

[9] J. G. Nagy, R. J. Plemmons and T. C. Torgersen, "Iterative image restoration using approximate inverse preconditioning," *IEEE Trans. on Image Proc.,* vol. 5, pp. 1151-1162, 1996.

[10] J. Nocedal and S. J. Wright, *Numerical Optimization,* Rensselaer, NY: Springer-Verlag, 1999.

[11] R. S. Frackowiak, K. J. Friston, C. D. Frith, R. J. Dolan and J. C. Mazziotta, *Human Brain Function,* New York: Academic Press, 1997.